

Accepted Manuscript

Quantum chemical studies on the partial hydrogenolysis of methyl 2,3-*O*-diphenylmethylene- α -l-rhamnopyranoside

Attila Mándi, István Komáromi, Anikó Borbás, Dezső Szikra, István P. Nagy, András Lipták, Sándor Antus

PII: S0040-4039(11)00039-6
DOI: [10.1016/j.tetlet.2011.01.021](https://doi.org/10.1016/j.tetlet.2011.01.021)
Reference: TETL 38957

To appear in: *Tetrahedron Letters*

Received Date: 10 November 2010
Revised Date: 17 December 2010
Accepted Date: 7 January 2011



Please cite this article as: Mándi, A., Komáromi, I., Borbás, A., Szikra, D., Nagy, I.P., Lipták, A., Antus, S., Quantum chemical studies on the partial hydrogenolysis of methyl 2,3-*O*-diphenylmethylene- α -l-rhamnopyranoside, *Tetrahedron Letters* (2011), doi: [10.1016/j.tetlet.2011.01.021](https://doi.org/10.1016/j.tetlet.2011.01.021)

This is a PDF file of an unedited manuscript that has been accepted for publication. As a service to our customers we are providing this early version of the manuscript. The manuscript will undergo copyediting, typesetting, and review of the resulting proof before it is published in its final form. Please note that during the production process errors may be discovered which could affect the content, and all legal disclaimers that apply to the journal pertain.

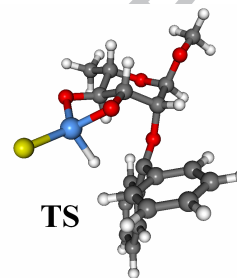
Graphical Abstract

Quantum chemical studies on the partial hydrogenolysis of methyl 2,3-*O*-diphenylmethylene- α -L-rhamnopyranoside

Attila Mándi, István Komáromi*, Anikó Borbás*, Dezső Szikra, István P. Nagy, András Lipták, Sándor Antus

The potential energy surface for dioxolane ring-opening and hydride donation for the title compound has been mapped. The transition state (TS) was determined at various levels of theories and it has been proven by intrinsic reaction coordinate calculations that it connects the reactant to the product.

Leave this area blank for abstract info.





Quantum chemical studies on the partial hydrogenolysis of methyl 2,3-*O*-diphenylmethylene- α -L-rhamnopyranoside

Attila Mándi^{a, b}, István Komáromi^{c, *}, Anikó Borbás^{a, *}, Dezső Szikra^d, István P. Nagy^d, András Lipták^a, Sándor Antus^{a, b}

^a Research Group for Carbohydrates of the Hungarian Academy of Sciences, H-4032, Debrecen, Hungary

^b Department of Organic Chemistry, University of Debrecen, H-4032, Debrecen, Hungary

^c Thrombosis, Haemostasis and Vascular Biology Research Group of the Hungarian Academy of Sciences, University of Debrecen, H-4032, Debrecen, Hungary

^d Department of Physical Chemistry, University of Debrecen, H-4032, Debrecen, Hungary

ARTICLE INFO

Article history:

Received

Received in revised form

Accepted

Available online

Keywords:

Diphenylmethylene acetal

Partial hydrogenolysis

Chloroalane

Mechanistic study

Quantum chemistry

ABSTRACT

The potential energy surface for dioxolane ring-opening and hydride donation for the title compound has been mapped. The transition state (TS) was determined at various levels of theories and it has been proven by intrinsic reaction coordinate calculations that it connects the reactant to the product. The breaking of the O3-C_{acetal} bond and formation of the new H-C bond seems to occur in one (rate limiting) elementary step, which is, however, rather asynchronous.

2010 Elsevier Ltd. All rights reserved.

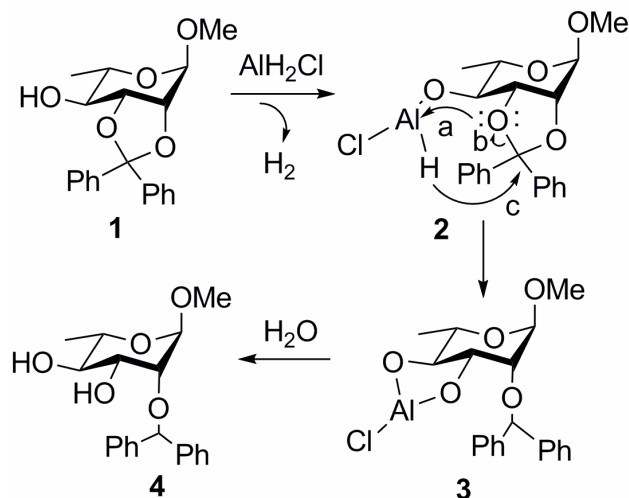
Lithium aluminium hydride (LAH) in combination with AlCl₃ as various “mixed hydride” reagents¹ is widely used for selective reductions in organic chemistry, especially in carbohydrate chemistry.² In the equilibrium reaction of LAH and AlCl₃ a mixture of alanes is formed. The main products are alane, chloroalane, and dichloroalane correspondingly to the 3 : 1, 1 : 1 and 1 : 3 LAH and AlCl₃ concentration ratios, while the side product is LiCl in every case. The acidity increases from alane towards AlHCl₂, while hydride-donating ability alters in an inverse manner.³ Although regioselective opening of cyclic benzylidene acetal derivatives with LAH and AlCl₃, or borane reduction is very important in carbohydrate chemistry, e.g. at 4,6-*O*-benzylidene acetals, only a few kinetic experiments^{4,5} and theoretical work⁵ (mainly dealing with electrostatic property calculations) can be found in the literature.

The reaction of methyl 2,3-*O*-diphenylmethylene- α -L-rhamnopyranoside derivatives with chloroalane in Et₂O : CH₂Cl₂ 1 : 1 has been studied by our research group.⁶ At the 4-OH derivative only the 2-*O*- diphenylmethyl product was formed, while in the 4-OMe or 4-deoxy cases the reaction resulted in a mixture of 2-*O*- and 3-*O*- ethers, where the latter were the major products. A schematic reaction mechanism was proposed for

compound **1** possessing a free hydroxy group at position 4,⁶ in which initially a 4-*O*-chloroalane derivative **2** forms then opening of the dioxolane ring takes place, and finally **3** is hydrolyzed to give **4** (Scheme 1). However, there were no proposals given on the sequence of elementary steps of the reaction.

Assuming that the formation of compound **2** is fast, compared to the formation of **3**, our goal was to investigate the second step of the proposed reaction mechanism. (The final hydrolytic reaction step is separable since it is initiated by addition of water) Thus a question arises: what is the order of the elementary bond rearrangements a-c in **2**? That is, do we have a multistep reaction with “stable” reaction intermediates or a single elementary step reaction? If the latter, is the sequence of bond rearrangements dominantly synchronous or asynchronous? These problems are addressed by means of theoretical methods. Due to the rather limited number of papers published so far on reactions of alane, and especially chloroalane derivatives,⁷ the basis and method dependency of the obtained results were investigated. This might be useful for researchers who are interested in the field of computational aluminum organic chemistry as well.

* Corresponding authors. Tel.: +36 52 512 900x55178; fax: +36 52 340 011 (I.K.); tel.: +36 52 512 900x22462; fax: +36 52 512 900x22342 (B.A.); e-mail addresses: komaromi@med.unideb.hu (I. Komáromi), borbasa@puma.unideb.hu (A. Borbás).

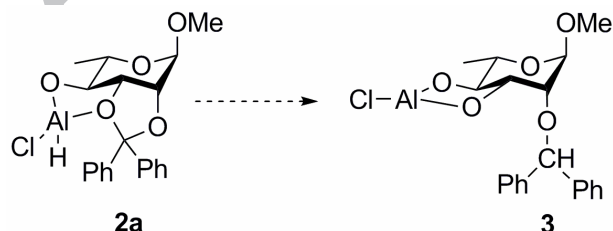


Scheme 1. Previous assumption on the mechanism of partial hydrogenolysis⁶

Geometry optimizations of **2** consistently lead to a structure in which the Al was strongly associated to O3. In fact, this association featured both minima found from relaxed rotation around the O4-Al bond. These two minima differ only in the configuration of the Al atom. The most stable (by ~9 kJ/mol) was that which also seemed to be more suitable for the next step regarding the orientation of the Al-H bond.

This geometry has interesting features. Consistently, at all the levels of theories we applied (Table S1 in the Supplementary data; the capital letter S indicates that the Figure or Table is available as Supplementary data) the Al-O3 bond distance was although only a little longer than the usual Al-O single bond (e.g. Al-O4), still substantially shorter than a simple van der Waals contact distance. It is not surprising since the three valenced Al has a hard character,⁸ and in close proximity the oxygen has unshared electron pairs. This oxygen now becomes three-coordinated which necessarily implicates weakened O-C bonds as demonstrated in Table S1 with substantially longer O3-CPh₂ than O2-CPh₂ bonds. It follows that bond formation between O3-Al in **2** is fast and precedes O3-CPh₂ bond breaking and hydride transfer. Therefore, we considered this four-coordinated Al compound in the rate limiting unimolecular reaction of dioxolane ring-opening as the “reactant”.

Regarding the geometry of the immediate product of dioxolane ring-opening (**3**), the Al now has two “normal” Al-O bonds of typical ~1.70-1.75 Å bond length. The Al, as expected, has a nearly planar local geometry. In this study we consider this molecule as the “product” since the subsequent step is hydrolysis which needs the addition of water and is separated in time, as well.⁶ This Letter deals with the “reactant” (**2a**) → “product” (**3**) reaction (Scheme 2).



Scheme 2. The structures of the “reactant” (**2a**) and the “product” (**3**)

In order to understand the mechanism of the ring-opening reaction, a two dimensional relaxed potential energy scan using the B3LYP/6-31G method was carried out along the breaking C-O and the newly forming C-H bonds as shown on Figure 1.

It is immediately apparent from Figure 1 that the “reactant” (**2a**) and “product” (**3**) can be connected on the surface through a single transition state (first order saddle point, **TS**). It is also apparent that the geometry in the local minimum corresponding to the starting molecule (**2a**) is remarkably flexible since a small change in energy can cause relatively large changes in the C-O or C-H internal coordinates. This is in an agreement with the fact that the “reactant” has weakened C-O3 and almost fully formed Al-O3 bonds which imparts increased flexibility for the H(Al) and O3 atoms relative to the acetal C. The slope of the product-side surface is substantially larger. This part of the surface can be characterized by a deep, long and narrow valley in which small changes in the C-H distance increases significantly the potential energy, while a large variation in the C-O bond distance has hardly any influence. (The potential surfaces at C-H distances smaller than 1.0 Å were not calculated, but it can be assumed that at those distances the energy values are rapidly increased) The reason is that once the C-O bond is broken the distance between these atoms can also be varied by rotation around the C2-O2 single bond.

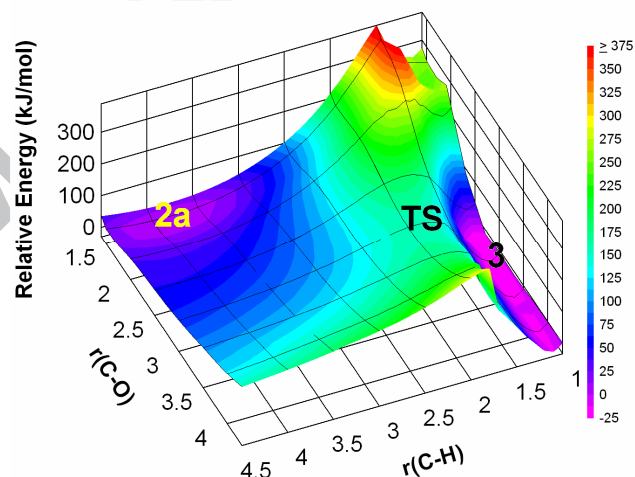


Figure 1. Potential energy surface at the B3LYP/6-31G level of theory as a function of the breaking $C_{\text{acetal}}\text{-O3}$ and the forming C-H(Al) bonds; energies and distances are given in kJ/mol and Å, respectively.

The transition state geometries and energies for this reaction starting from the **TS** geometry on the potential energy surfaces (Figure 1) were determined at numerous levels of theory, and the results along with the corresponding values for reactant and product are summarized in Table S1. The most obvious feature of the values listed in this table is that the corresponding geometrical parameters are almost independent of the applied levels of theories. Comparing the “reactant” and “product” geometries to the **TS** geometries, it is immediately apparent that the **TS** C-O3 bond distance is “product-like”, while the distance between the acetal C and the transferred hydride anion is close to the arithmetic mean of the corresponding distances at the “reactant” and “product”. Relatively smaller changes were observed in the Al-O3 bond length distances during the reaction, in agreement with the aforementioned “end point” values. The changes are probably mainly due to alteration in the coordination number of the Al atom. The changes in other inter-atomic distances are less remarkable during the hydride anion transfer reaction.

While all the theoretical methods applied for the reaction showed similar transition state geometries, rather large differences were observed in the predicted TS energies. Consistently 125-130 kJ/mol zero point vibrational energy corrected activation energies were obtained by the DFT methods. The HF methods, since they neglect the correlation energy, which is usually larger at the transition state geometries, show the highest TS energies in agreement with the observations.⁹ The MP2 and ONIOM methods resulted in energies which were between the B3LYP and HF methods comparing the values calculated at the same basis set.

Independently from the levels of approximation (HF, DFT, MP2 and ONIOM using either MP4(SDQ) or QCISD levels of theory for the model system) and the basis sets (ranging from 6-31G to 6-311++G(d,p)) the obtained TSs have a common feature, namely that the C-O bond breaking precedes C-H bond formation. Graphical representations of these species and the energy profile of the reaction calculated at the B3LYP/6-311+G(d,p) level of theory are shown in Figure 2.

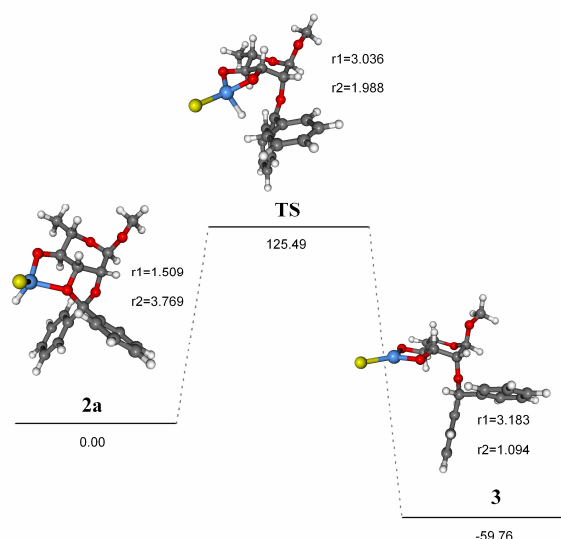


Figure 2. Reaction profile based upon the B3LYP/6-311+G(d,p) calculations; r1 is the C-O breaking distance while r2 is the forming C-H; energies and distances are given in kJ/mol and Å, respectively.

Although the intrinsic reaction path¹⁰ was only followed at the B3LYP/6-31G(d) level of theory, presumption of a similar reaction path seems to be plausible for all the theoretical methods we applied. This can be justified by the predicted similar transition state as well as product and the reactant geometries obtained at all levels of theory (Tables S1 and S2).

Regarding the energy profile and inter-atomic distances as a function of mass-weighted Cartesian intrinsic reaction coordinate,¹⁰ both the asymmetric energy profile and the asynchronous nature of bond rearrangement can be observed (Figure 3). The latter is straightforward from Figure 3B comparing the C-H (newly forming bond) and C-O (breaking bond) curves, since the C-O bond is practically broken when the C-H bond begins to form. It is noteworthy that the Al-O bond is almost insensitive to the reaction coordinate values, only a marginal shortening is observable. It should also be mentioned that geometry optimizations from the negative and positive end points of the intrinsic reaction coordinates lead to the reactant and to the product, respectively. The atomic movements at the transition state corresponding to the imaginary frequency is shown in the Supplementary data, Movie 1.

From these calculations the theoretical zero point vibrational energy corrected TS energies were extracted. The rates of chemical reactions at constant pressure, however, were related to the Gibbs free activation energy. Nevertheless, since the reaction we calculated is an intermolecular bond rearrangement, neither a substantial entropy effect nor substantial volume changes are expected. Comparison the calculated gas phase free energy difference (129.9 kJ/mol) differs only marginally from the ZPVE corrected electronic energy difference (125.5 kJ/mol) at the B3LYP/6-311+G(d,p) level of theory. It should be noted, however, that considering the low frequency modes as harmonic vibrations can cause relatively large errors in the calculated free energy value.

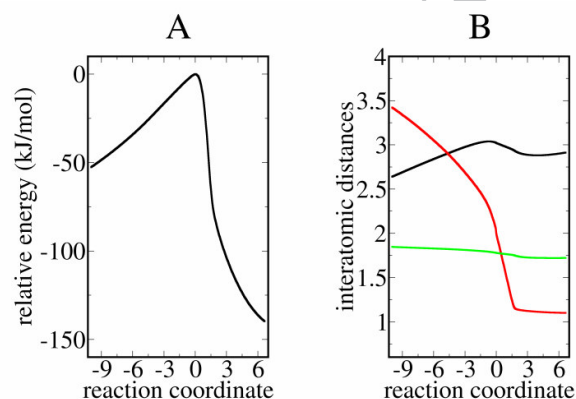
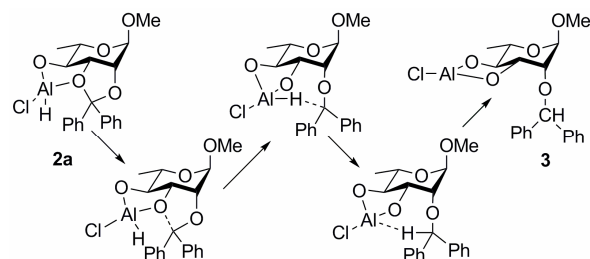


Figure 3. Reaction energy profile (A), and Al-O (green), C-O (black) and C-H (red) interatomic distances (B) as a function of the intrinsic reaction coordinate calculated at the B3LYP/6-311G(d) level of theory. The zero reaction coordinate value corresponds to the transition state. Distances are in Å and energies are in kJ/mol.

Furthermore, it was shown above that during the 2→3 reaction the C-O bond breaking precedes C-H bond formation, and the transition state corresponds dominantly to a hydride anion transfer. For such systems the contribution of the tunnelling effect¹¹ is usually non-negligible.

Nevertheless, based on the theoretical calculations a modified reaction mechanism can be proposed for the dioxolane ring opening. Starting from the 4-O-chloroalane derivative the first step is the strong (almost fully-formed single bond) interaction between the Al and O3 atoms which implicates some bond weakening of O3-C3, and especially the O3-C_{acetal} bonds. This compound can be considered as a relatively stable reaction intermediate. It follows a single step reaction which is, however, strongly asynchronous. First, the C-O bond practically breaks and then C-H bond formation begins. This mechanism is summarized in Scheme 3.



Scheme 3. Mechanism of the rate determining step of the partial hydrogenolysis reaction according to the computational results

There is certain analogy between this reaction and the reductive acetal cleavage studied by Saito et al.¹² In both cases the reductive reagent is coordinated to the free hydroxyl group which is in close proximity to the reaction center. It increases the probability to form the strongly polar („intimate ion pair”^{13,14}) intermediates and TS(s) which are assumed to play crucial roles in the reactions. In our case the Et₂O presumably reduces the hard character of chloroalane and this way decreases the probability of side-reactions as discussed by Johnsson et al.^{4b} The reaction studied here shows similarities to the reaction of optically active 2,3-butanediol-acetals where one of the oxygen lone pair bears Lewis acid („type A” compounds and Scheme III reaction according to the classification given by Denmark et al.¹⁴).

Finally, on the basis of the numerous calculations at different levels of theory [HF/6-31G to B3LYP/6-311++G(d,p) or ONIOM QCISD/6-31++G(d,p):B3LYP/6-31G(d)], a conclusion can be drawn that the B3LYP/6-31G(d) method is an economic and still accurate compromise in the computational chemistry of large organic chloroalane derivatives.

In conclusion, we have modeled the dioxolane ring-opening reaction of methyl 2,3-*O*-diphenylmethyle- α -L-rhamnopyranoside induced by addition of LiAlH₄ and AlCl₃. Starting from the proposed 4-*O*-chloroalane derivative, we found that the Al coordinates spontaneously to the O3 atom leading to weakening of the O3-C_{acetal} bond. The potential energy surface of the reaction defined by the breaking O3-C_{acetal} and forming H-C bonds was then mapped. The end points of this reaction (**2a** and **3**) and the single TS connecting them (proved by following the minimal energy path) were determined at various levels of theory. We found that **3** forms from **2a** in a single elementary reaction step, which is, however, strongly asynchronous. We have also shown that the economic B3LYP/6-31G(d) method (and therefore probably all gradient-corrected DFT methods with suitable functional) can be used in modelling reactions of large aluminum organic compounds.

Geometry optimizations, transition state calculations, potential energy surface scan, 2nd derivative calculations and intrinsic reaction coordinate calculations were carried out using the Gaussian 03¹⁵ package. Transition state- and minimum energies were corrected with the zero point vibrational energy at the same level of theory as used for optimizations. The existence of a first order saddle point (transition state) and minima were proved by either one or no imaginary frequencies, respectively. The exceptions were the MP2/6-31G(d,p), MP2/6-31++G(d,p), B3LYP/6-311++G(d,p) and ONIOM methods¹⁶ in which QCISD and MP4(SDQ) calculations were used in “high level” calculations for the model system. The definition of the model- and the real system is shown in Figure S1. Starting from the transition state geometry the mass-weighted Cartesian intrinsic reaction coordinate (IRC) method was used at B3LYP/6-31G(d) level of theory to follow the minimum energy path (MEP) and to prove that the transition state connects the reactant to the product. Visualization was carried out using Molekel,¹⁷ Chimera,¹⁸ DPlot¹⁹ and Grace²⁰ software.

Acknowledgements

The Hungarian National Infrastructure Development Program (NIIF 1116), the Hungarian Scientific Research Funds (OTKA NK-68578, K-62802 and TÁMOP 4.2.1/B-09/1/KONV-2010-0007) supported this work.

Supplementary data

Supplementary data (the main parameters of end point and TS geometries, energies, zero point vibrational energy corrected transition state energies as well as the imaginary frequencies of TS calculated at various levels of theory are listed in Table S1. All the Cartesian coordinates of the geometries given in Table S1 as well as the corresponding energies are listed in Table S2. The ONIOM partition scheme is shown in Figure S1. Movie S1 demonstrates the movements corresponding to the imaginary frequency) associated with this article can be found, in the online version, at doi:

References and notes

1. Ashby, E. C.; Prather, J. *J. Am. Chem. Soc.* **1966**, *88*, 729-733.
2. Lipták, A.; Jodál, I.; Nánási, P. *Carbohydr. Res.* **1975**, *44*, 1-11.
3. Ashby, E. C.; Cooke, B. *J. Am. Chem. Soc.* **1968**, *90*, 1625-1630.
4. (a) Johnsson, R.; Cukalevski, R.; Dragen, F.; Ivanisevic, D.; Johansson, I.; Petersson, L.; Wettergren, E. E.; Yam, K. B.; Yang, B.; Ellervik, U. *Carbohydr. Res.* **2008**, *343*, 2997-3000; (b) Johnsson, R.; Ohlin, M.; Ellervik, U. *J. Org. Chem.* **2010**, *75*, 8003-8011.
5. Johnsson, R.; Olsson, D.; Ellervik, U. *J. Org. Chem.* **2008**, *73*, 5226-5232.
6. Hajkó, J.; Borbás, A.; Szabovik, G.; Kajtár-Peredy, M.; Lipták, A. *J. Carbohydr. Chem.* **1997**, *16*, 1123-1144.
7. (a) Swihart, M. T.; Catoire, L. *J. Phys. Chem. A* **2001**, *105*, 264-273; (b) Himmel, H. J.; Klaus, C. Z. *Anorg. Allg. Chem.* **2003**, *629*, 1477-1484; (c) Bundens, J. W.; Seida, P. R.; Jeyakumar, D.; Franci, M. M. *J. Mol. Graph. Model.* **2005**, *24*, 195-202.
8. Pearson, R. G. *J. Am. Chem. Soc.* **1963**, *85*, 3533-3539.
9. (a) Levine, I. N. *Quantum Chemistry*, Pearson Prentice Hall, Upper Saddle River, 2009, pp. 700-718; (b) Komáromi, I.; Tronchet, J. M. J. *J. Phys. Chem. A* **1997**, *101*, 3554-3560; (c) Zheng, J. J.; Zhao, Y.; Truhlar, D. G. *J. Chem. Theory Comput.* **2007**, *3*, 569-582.
10. (a) Gonzalez, C.; Schlegel, H. B. *J. Chem. Phys.* **1991**, *95*, 5853-5860; (b) Schlegel, H. B. *J. Chem. Soc. Faraday Trans.* **1994**, *90*, 1569-1574.
11. Kuhn, H.; Försterling, H. D. *Principles of Physical Chemistry*, John Wiley & Sons, Chichester, 2000, pp. 687-689.
12. Saito, S.; Kuroda, A.; Tanaka, K.; Kimura, R. *Synlett* **1996**, 231-233.
13. Winstein, S.; Clippinger, E.; Fainberg, A. H.; Heck, R.; Robinson, G. C. *J. Am. Chem. Soc.* **1956**, *78*, 328-335.
14. Denmark, S. E.; Almstead, N. G. *J. Am. Chem. Soc.* **1991**, *113*, 8089-8110.
15. Frisch, M. J.; Trucks, G. W.; Schlegel, H. B.; Scuseria, G. E.; Robb, M. A.; Cheeseman, J. R.; Montgomery, Jr., J. A.; Vreven, T.; Kudin, K. N.; Burant, J. C.; Millam, J. M.; Iyengar, S. S.; Tomasi, J.; Barone, V.; Mennucci, B.; Cossi, M.; Scalmani, G.; Rega, N.; Petersson, G. A.; Nakatsuji, H.; Hada, M.; Ehara, M.; Toyota, K.; Fukuda, R.; Hasegawa, J.; Ishida, M.; Nakajima, T.; Honda, Y.; Kitao, O.; Nakai, H.; Klene, M.; Li, X.; Knox, J. E.; Hratchian, H. P.; Cross, J. B.; Bakken, V.; Adamo, C.; Jaramillo, J.; Gomperts, R.; Stratmann, R. E.; Yazyev, O.; Austin, A. J.; Cammi, R.; Pomelli, C.; Ochterski, J. W.; Ayala, P. Y.; Morokuma, K.; Voth, G. A.; Salvador, P.; Dannenberg, J. J.; Zakrzewski, V. G.; Dapprich, S.; Daniels, A. D.; Strain, M. C.; Farkas, O.; Malick, D. K.; Rabuck, A. D.; Raghavachari, K.; Foresman, J. B.; Ortiz, J. V.; Cui, Q.; Baboul, A. G.; Clifford, S.; Cioslowski, J.; Stefanov, B. B.; Liu, G.; Liashenko, A.; Piskorz, P.; Komaromi, I.; Martin, R. L.; Fox, D. J.; Keith, T.; Al-Laham, M. A.; Peng, C. Y.; Nanayakkara, A.; Challacombe, M.; Gill, P. M. W.; Johnson, B.; Chen, W.; Wong, M. W.; Gonzalez, C.; Pople, J. A. *Gaussian 03*, Revision C.02. 2004, Gaussian Inc., Wallingford CT.
16. Dapprich, S.; Komáromi, I.; Byun, K. S.; Morokuma, K.; Frisch, M. J. *J. Mol. Struct. (Theorchem)* **1999**, *462*, 1-21.
17. Flückiger, P.; Lüthi, H. P.; Portmann, S.; Weber, J. *MOLEKEL* **5.4.**, 2000-2002, Swiss Center for Scientific Computing, Manno, Switzerland.

-
18. Pettersen, E. F.; Goddard, T. D.; Huang, C. C.; Couch, G. S.; Greenblatt, D. M.; Meng, E. C.; Ferrin, T. E. *J. Comput. Chem.* **2004**, 25, 1605-1612.
 19. <http://www.dplot.com/index.htm>
 20. <http://plasma-gate.weizmann.ac.il/Grace/>